

General Disclaimer

One or more of the Following Statements may affect this Document

- This document has been reproduced from the best copy furnished by the organizational source. It is being released in the interest of making available as much information as possible.
- This document may contain data, which exceeds the sheet parameters. It was furnished in this condition by the organizational source and is the best copy available.
- This document may contain tone-on-tone or color graphs, charts and/or pictures, which have been reproduced in black and white.
- This document is paginated as submitted by the original source.
- Portions of this document are not fully legible due to the historical nature of some of the material. However, it is the best reproduction available from the original submission.



Programs for Calculating Quasi-Three-Dimensional Flow in a Turbomachine Blade Row

(NASA-TM-83588) PROGRAMS FOR CALCULATING
QUASI-THREE-DIMENSIONAL FLOW IN A
TURBOMACHINE BLADE ROW (NASA) 22 p
HC A02/MF A01

N84-17138

CSSL 01A

Unclas
18339

G3/02

Theodore Katsanis
Lewis Research Center
Cleveland, Ohio

Prepared for the
Computational Fluid Dynamics User's Workshop
sponsored by the University of Tennessee Space Institute
Tullahoma, Tennessee, March 12-16, 1984

NASA

PROGRAMS FOR CALCULATING QUASI-THREE-DIMENSIONAL FLOW
IN A TURBOMACHINE BLADE ROW

Theodore Katsanis

National Aeronautics and Space Administration
Lewis Research Center
Cleveland, Ohio 44135

INTRODUCTION

The design of blades for compressors and turbines ideally requires methods for analyzing unsteady, three-dimensional, turbulent viscous flow through a turbomachine. Clearly, such solutions are impossible at the present time, even on the largest and fastest computers. The usual approach at present is to analyze only steady flows and to separate inviscid solutions from viscous solutions. Three-dimensional inviscid solutions are beginning to be obtained with the present generation of computers, but they require excessive computer time. So, at present, inviscid analyses usually involve a combination of several two-dimensional solutions on intersecting families of stream surfaces to obtain what is called a quasi-three-dimensional solution.

Since there are several choices of two-dimensional surfaces to analyze and many ways of combining them, there are many approaches to obtaining a quasi-three-dimensional solution. Most two-dimensional solutions are either on a blade-to-blade surface of revolution (Wu's S_1 surface, ref. 1) or on the meridional or midchannel stream surface between two blades (Wu's S_2 surface). However, when three-dimensional effects are most important, significant information can often be obtained from a solution on a passage cross sectional surface (normal to the flow). This is called a channel solution (fig. 1).

In the MERIDL program (refs. 4 and 5) a solution to the equations of flow on the meridional S_2 surface is carried out. This solution surface is chosen when the turbomachine under consideration has significant variation in flow properties in the hub-shroud direction, especially when input is needed for use in blade-to-blade calculations. The solution can be obtained either by the quasi-orthogonal method, which solves the velocity-gradient equation from hub to shroud on the meridional stream surface (ref. 2), or by a finite-difference method, which solves a finite-difference equation for stream function on the same stream surface. The quasi-orthogonal method is efficient in many cases and can obtain solutions into the transonic regime. However, there is difficulty in obtaining a solution when blade aspect ratios are above 1. Difficulties are also encountered with curved passages and low-hub-tip-ratio blades. For such cases, the most promising method is the stream-function finite-difference solution, which is limited to subsonic flows.

Stream-function finite-difference programs for flow on the midchannel surface of a turbomachine have been reported in the literature. However, many of these programs are proprietary or are of limited generality. MERIDL is very general and has been thoroughly tested and refined as the result of extensive usage at the NASA Lewis Research Center and by industry.

MERIDL was written for an axial-, mixed-, or radial-flow turbomachine blade row, either a compressor or turbine, or for an annular duct. Upstream

and downstream flow conditions can vary from hub to shroud. The solution is for compressible, subsonic flow or for incompressible flow. An approximate correction for loss of stagnation pressure through the blade row is provided. The blade row may be either fixed or rotating. The blades may be twisted and leaned and can have high aspect ratio and arbitrary thickness distribution.

The solution obtained by MERIDL also provides the information necessary for a more detailed blade-shape analysis of blade-to-blade surfaces (fig. 1). A useful program for this purpose is TSONIC (ref. 3). Information needed to prepare all the input for TSONIC is calculated and printed by MERIDL, and is stored in the required input format for TSONIC.

SYMBOLS

B tangential space between blades, rad
 b stream-channel thickness normal to meridional streamline, meters
 C_p specific heat at constant pressure, J/(kg)(K)
 F^p vector normal to midchannel stream surface and proportional to tangential pressure gradient, N/kg
 m meridional streamline distance, meters
 p pressure, N/meter²
 R gas constant, J/(kg)(K)
 r radius from axis of rotation, meters
 s distance along orthogonal mesh lines in throughflow direction, meters
 T temperature, K
 t distance along orthogonal mesh lines in direction across flow
 u normalized stream function
 V absolute fluid velocity, meters/sec
 W fluid velocity relative to blade, meters/sec
 w mass flow, kg/sec
 z axial coordinate, meters
 α angle between meridional streamline and axis of rotation, rad; see fig. 4
 β angle between relative velocity vector and meridional plane, rad; see fig. 4
 ζ coefficient in stream-function equation, defined in eq. (3)
 θ relative angular coordinate, rad; see fig. 4
 ξ coefficient in stream-function equation, defined in eq. (2)
 ρ density, kg/meter³
 φ angle between s-distance line and axis of rotation, rad; see fig. 3
 ω rotational speed, rad/sec; see fig. 4

Subscripts:

m component in direction of meridional streamline
 s component in s-direction
 t component in t-direction
 z component in axial direction
 θ component in tangential direction

Superscripts:

' absolute stagnation condition
 " relative stagnation condition

METHOD OF ANALYSIS

Basic Assumptions for MERIDL

It is desired to determine the flow distribution through a stationary or rotating cascade of blades on a midchannel hub-shroud stream surface. The following simplifying assumptions are used in deriving the equations and in obtaining a solution:

- (1) The flow relative to the blade is steady.
- (2) The fluid is a perfect gas with constant specific heat C_p .
- (3) The only forces along a hub-shroud orthogonal mesh line are those due to momentum and pressure gradient.
- (4) There is no heat transfer.
- (5) The midchannel surface is a stream surface that has the same shape as the blade mean-camber surface, except near the leading and trailing edges, where an arbitrary correction is made to match the free-stream flow.
- (6) The velocity varies linearly between blade surfaces.
- (7) The relative stagnation pressure loss is known through the blade row.
- (8) The upstream and downstream boundaries of the solution region are orthogonal to the streamlines.

The flow may be axial, mixed, or radial. Whirl (rV_θ), stagnation pressure, and stagnation temperature may vary from hub to shroud, both upstream and downstream of the blade row. The blade row may be either fixed or rotating, with leaned and twisted blades; or there may be no blades at all. Within the given assumptions, no terms are omitted from the equations.

In connection with assumption 3, the viscous forces along a hub-shroud orthogonal mesh line are neglected, since these forces are usually very small. The viscous forces in the streamwise direction are much larger. The effects of these streamwise viscous forces are considered indirectly by specifying a streamwise total-pressure-loss distribution.

MERIDL Stream-Function Solution

The cylindrical coordinate system is shown in figure 4. However, the solution is obtained on an orthogonal mesh, as illustrated in figure 3. The variables s and t are used to denote distance along the streamwise and normal orthogonals, respectively. The stream function satisfies the following equation (ref. 4):

$$\frac{\partial^2 u}{\partial s^2} + \frac{\partial^2 u}{\partial t^2} - \frac{\partial u}{\partial s} \left(\frac{\sin \varphi}{r} + \frac{1}{B} \frac{\partial B}{\partial s} + \frac{1}{\rho} \frac{\partial \rho}{\partial s} - \frac{\partial \varphi}{\partial t} \right) - \frac{\partial u}{\partial t} \left(\frac{\cos \varphi}{r} + \frac{1}{B} \frac{\partial B}{\partial t} + \frac{1}{\rho} \frac{\partial \rho}{\partial t} + \frac{\partial \varphi}{\partial s} \right) + \frac{rB\rho}{wW_s} \left[\frac{w_\theta}{r} \frac{\partial (rV_\theta)}{\partial t} + \xi W^2 + \zeta + F_t \right] = 0 \quad (1)$$

where

ORIGINAL PAGE IS
OF POOR QUALITY

$$\xi = \frac{1}{2} \left(\frac{R}{C_p p''} \frac{\partial p''}{\partial t} - \frac{1}{T''} \frac{\partial T''}{\partial t} \right) \quad (2)$$

$$\zeta = \omega^2 r \cos \varphi - \frac{RT''}{p''} \frac{\partial p''}{\partial t} \quad (3)$$

$$F_t = \frac{\partial \theta}{\partial t} \frac{1}{\rho} \frac{\partial p}{\partial \theta} \quad (4)$$

The derivatives of the stream function satisfy the equations

$$\frac{\partial u}{\partial s} = - \frac{r B \rho W_t}{w} \quad (5)$$

$$\frac{\partial u}{\partial t} = \frac{r B \rho W_s}{w} \quad (6)$$

The stream-function equation (1) is a partial differential equation on a midchannel hub-shroud stream surface (assumption 5). It is in one unknown (the stream function) as a function of two variables and is derived from Wu's momentum equation (eq. (96), ref. 1) on what he calls an S_2 surface. Equation (1) is nonlinear but can be solved iteratively by the finite-difference method when the flow is completely subsonic.

A finite region (as indicated in fig. 2) is considered for the solution of equation (1). It is assumed that the upstream and downstream boundaries are sufficiently far from the blade so as to have a negligible effect on the solution. Equation (1) is elliptic for subsonic flow. Therefore, when the flow is entirely subsonic, equation (1) can be solved when proper boundary conditions are specified on the entire boundary of the region. These conditions are the values of the stream function or its normal derivative on all four boundaries. The stream function is zero on the hub and 1 at the shroud. On the upstream and downstream boundaries, the derivative of the stream function normal to the boundary is assumed to be zero. This is equivalent to assuming that the upstream and downstream boundaries are orthogonal to the streamlines (assumption 8).

The numerical solution of equation (1) is obtained by the finite-difference method. A grid must be used for the finite-difference equations. The type of grid that was chosen is an orthogonal mesh that is generated by the program. The space between the hub and the shroud is divided into equal increments along several hub-shroud lines. Spline curves are then fit through the resulting points to obtain the streamwise orthogonals (fig. 3). The normal orthogonals are obtained by a predictor-corrector technique. This technique is analogous to the second-order Runge-Kutta method for solving ordinary differential equations, which is known also as the improved Euler method or Heun's method (ref. 6). The distances along orthogonal mesh lines are s and t . The s -distance is in the streamwise direction and the t -distance is normal to this, as indicated in figure 3. With the mesh determined, the finite-

difference equations on the orthogonal mesh are given in reference 5. Note that the orthogonal mesh is not used as a coordinate system.

The finite-difference equations are nonlinear since the original equation (1) is nonlinear. These equations can be solved iteratively. On the first iteration an initial density is assumed; this linearizes some of the terms. The remaining nonlinear terms are omitted for the first iteration so that the finite-difference equations are entirely linearized. These linearized equations are then solved to obtain the first approximate solution for the stream function. This solution provides information that is used to obtain a better estimate of the density and an estimate of the other nonlinear terms. The equations are then solved again to obtain an improved solution. This process is repeated, and by iteration a final converged solution can be obtained if the flow is subsonic.

For each step of this iteration the linearized finite-difference equations must be solved. The method used to solve the equations is successive over-relaxation (ref. 7) with an optimum overrelaxation factor. Since this is also an iterative method, we have two levels of iteration. The overrelaxation is performed in the "inner iteration," and the corrections to the nonlinear terms are made in the "outer iteration." The inner iteration is internal to the program, so the only iteration apparent to the user is the outer iteration.

After the stream function is obtained, the velocity distribution is found by numerical partial differentiation of the stream function and by using equations (5) and (6). The details of the numerical procedure and programming technique are described in reference 5.

Application of MERIDL

MERIDL can be used both for analysis and as a design tool. When it is used for design, other programs should be used with MERIDL. For axial compressors, reference 8 describes a program that will give blade mean-camber line coordinates and thicknesses for an axial compressor blade. This blade design can be checked by using the MERIDL program to analyze the flow distribution in detail. Usually, changes must be made to the blade design to achieve a desirable flow distribution. These changes may involve more than just the blade shape; for example, hub and shroud profile, inlet and outlet whirl (rV_θ) distribution, and loss distribution may have to be changed. Of course, the accuracy of the MERIDL solution depends on the accuracy of the boundary conditions used.

When a reasonable flow pattern is achieved by the MERIDL flow analysis on the midchannel stream surface, more detailed blade surface velocities can be obtained by flow analyses on various blade-to-blade stream surfaces. A useful program for this purpose is TSONIC (ref. 3). All of the information required to compute input for TSONIC is calculated and printed directly by MERIDL. Further changes in blade shape or whirl distribution may be considered at this time. Reference 9 (ch. VII) gives information on incidence and deviation for good designs and for off-design conditions.

For cases where the flow is well guided in the channel but has large variations, both from blade to blade and from hub to shroud, the CHANEL program (ref. 10) is useful. The CHANEL program obtains a solution on a channel cross-section surface. The CHANEL program is particularly useful for calculating choking mass flow through a blade row.

Basic Assumptions for TSONIC

The simplifying assumptions used are those in references 11 and 12. These assumptions are

- (1) The flow is steady relative to the blade.
- (2) The fluid is a perfect gas (constant C_p) or is incompressible.
- (3) The fluid is nonviscous, and there is no heat transfer (therefore, the flow is isentropic).
- (4) The flow is absolutely irrotational.
- (5) The blade-to-blade surface is a surface of revolution. (This does not exclude straight infinite cascades.)
- (6) The velocity component normal to the blade-to-blade surface is zero.
- (7) The stagnation temperature is uniform across the inlet.
- (8) The velocity magnitude and direction are uniform across both the up-stream and downstream boundaries.
- (9) The only forces are those due to momentum and pressure gradient.

The flow may be axial, radial, or mixed and there may be a variation in the normal stream-channel thickness b in the through-flow direction. A loss in relative stagnation pressure can be specified.

TSONIC Stream-Function Solution

The notation for velocity components is shown in figure 4. For generality, the meridional streamline distance m is used as an independent coordinate (see fig. 5). Thus, m and θ are the two basic independent variables. A stream channel is defined by specifying a meridional streamline radius r and a stream-channel thickness b as functions of m alone (see fig. 6). The variables r and b are constant functions of θ .

For the mathematical formulation of the problem the stream function is used. The stream function u is normalized so that u is 0 on the upper surface of the lower blade, and 1 on the lower surface of the upper blade. The stream function satisfies the following equation (ref. 11).

$$\frac{1}{r^2} \frac{\partial^2 u}{\partial \theta^2} + \frac{\partial^2 u}{\partial m^2} - \frac{1}{r^2} \frac{1}{\rho} \frac{\partial \rho}{\partial \theta} \frac{\partial u}{\partial \theta} + \left[\frac{\sin \alpha}{r} - \frac{1}{b\rho} \frac{\partial(b\rho)}{\partial m} \right] \frac{\partial u}{\partial m} = \frac{2b\rho\omega}{w} \sin \alpha \quad (7)$$

The derivatives of the stream function satisfy

$$\frac{\partial u}{\partial m} = - \frac{b\rho}{w} W_\theta \quad (8)$$

$$\frac{\partial u}{\partial \theta} = \frac{b\rho r}{w} W_m \quad (9)$$

If the flow is entirely subsonic, equation (7) is elliptic. Boundary conditions for the entire boundary ABCDEFGHA of figure 7 will determine a unique solution for u . These boundary conditions (ref. 11) are as follows:

Boundary segment	Boundary condition
AB	u is 1 less than the value of u on GH at the same m coordinate
BC	$u = 0$
CD	u is 1 less than the value of u on EF at the same m coordinate
DE	$\left(\frac{\partial u}{\partial n}\right)_{out} = -\frac{\tan \beta_{out}}{sr_{out}}$
EF	u is 1 greater than the value of u on CD at the same m coordinate
FG	$u = 1$
GH	u is 1 greater than the value of u on AB at the same m coordinate
AH	$\left(\frac{\partial u}{\partial n}\right)_{in} = \frac{\tan \beta_{in}}{sr_{in}}$

NUMERICAL EXAMPLES

AXIAL Turbine

A goal of small-turbine research at the NASA Lewis Research Center is to investigate concepts that offer the potential for reducing secondary flows and increasing turbine efficiency. One concept that has this potential is stator endwall contouring. To provide better understanding of the loss mechanisms associated with stator contouring, a program was conducted at Lewis to design and evaluate, experimentally and analytically, contoured stator-endwall designs for a 12.77-cm-tip-diameter axial-flow turbine (ref. 13) as compared with a cylindrical stator-endwall design. The analysis method used MERIDL and TSONIC to calculate the blade surface and endwall velocities. Then a boundary layer program, BLAYER (ref. 14) was used to calculate stator and rotor displacement and momentum thickness, which are then used to calculate profile friction losses (including mixing loss) and endwall friction losses. Additional published correlations are used to calculate losses due to incidence, secondary flow, rotor tip clearance, disk windage, and exhaust duct friction between rotor trailing edge and the downstream measuring station.

Figure 8 shows a cross section of the turbine, and figure 9 shows the stators that were analyzed and tested. The design blade-surface-velocity distributions calculated by MERIDL and TSONIC are shown in figure 10. There were no static pressure taps on the stator or rotor blades, so only a comparison of computed and experimental velocities and flow angles at the stator exit and rotor exit could be made. Reference 13 shows very good agreement between analytical and experimental velocities and flow angles at the mean section of all three stator-rotor configurations. At the hub and tip sections the degree of comparison is not as good. This is not unexpected since MERIDL is an inviscid program which calculates flow conditions along a hub-to-shroud midchannel stream surface. Factors such as endwall boundary layer skewing and three-

dimensional tip clearance effects are not accounted for. However, based on the overall degree of comparison between the analytical and experimental flow conditions it was felt that a valid loss assessment could be made. The computed efficiencies were slightly higher than their respective experimentally measured values. However, the increases in computed stage efficiency for the contoured stators compared to the cylindrical stator was quite close. Although there was no comparison of surface velocities or pressures for these stators, reference 15 shows extensive experimental comparisons for another stator.

For practical applications it is important to know the efficiency of a turbine over a range of speeds and pressure ratios, not just at the design point. The above described analysis has been used to calculate efficiency for this turbine at 80 to 100 percent speed and over a range of pressure ratios. The predictions are compared with experimental results in figure 11. Further details are reported in reference 16.

Fan Stator

References 17 and 18 report experimental performance results and analytical code calculations for three fan stator designs. These studies were done in support of NASA's low-noise, conventional aircraft engine performance. Figure 12 shows the flow path for the stage, and figure 13 shows the calculated surface velocities for three different stators. Experimental comparisons for the surface velocities are not available for these stators. The parameter of interest in the calculations was the ratio $V_{\max,ss}/V_{TE}$ as shown in figure 13. According to reference 18, this ratio correlated the experimentally measured total-loss parameter over a wide range of flows from minimum-loss to near-stall operation and for all stators and speeds studied.

REFERENCES

1. Wu, Chung-Hua: A General Theory of Three-Dimensional Flow in Subsonic and Supersonic Turbomachines of Axial-, Radial-, and Mixed-Flow Types. NACA TN-2604, 1952.
2. Katsanis, T.: Use of Arbitrary Quasi-Orthogonals for Calculating Flow Distribution in the Meridional Plane of a Turbomachine. NASA TN D-2546, 1964.
3. Katsanis, T.: FORTRAN Program for Calculating Transonic Velocities on a Blade-to-Blade Stream Surface of a Turbomachine. NASA TN D-5427, 1969.
4. Katsanis, T.; and McNally, W. D.: Revised FORTRAN Program for Calculating Velocities and Streamlines on the Hub-Shroud Mid-Channel Stream Surface of an Axial-, Radial-, or Mixed-Flow Turbomachine or Annular Duct. I - User's Manual. NASA TN D-8430, 1977.
5. Katsanis, T.; and McNally, W. D.: Revised FORTRAN Program for Calculating Velocities and Streamlines on the Hub-Shroud Midchannel Stream Surface of an Axial-, Radial-, or Mixed-Flow Turbomachine or Annular Duct. II - Programmer's Manual. NASA TN D-8431, 1977.
6. McCracken, Daniel D.; and Dorn, William S.: Numerical Methods and FORTRAN Programming. John Wiley and Sons, 1964.
7. Varga, Richard S.: Matrix Iterative Analysis. Prentice-Hall, 1962.
8. Crouse, J. E.: Computer Program for the Definition of Transonic Axial Flow Compressor Blade Rows. NASA TN D-7345, 1974.
9. Johnson, Irving A.; and Bullock, Robert O., eds.: Aerodynamic Design of Axial-Flow Compressors. NASA SP-36, 1965.

10. Katsanis, T.: FORTRAN Program for Quasi-Three-Dimensional Calculation of Surface Velocities and Choking Flow for Turbomachine Blade Rows. NASA TN D-6177, 1971.
11. Katsanis, T.; and McNally, W. D.: FORTRAN Program for Calculating Velocities and Streamlines on a Blade-to-Blade Stream Surface of a Tandem Blade Turbomachine. NASA TN D-5044, 1969.
12. Katsanis, T.; and McNally, W. D.: Revised FORTRAN Program for Calculating Velocities and Streamlines on a Blade-to-Blade Stream Surface of a Turbomachine. NASA TM X-1764, 1969.
13. Haas, Jeffrey E.; and Boyle, Robert J.: Analytical and Experimental Investigation of Stator Endwall Contouring in a Small Axial-Flow Turbine. II - Stage Results. Prepared NASA Technical Paper.
14. McNally, W. D.: FORTRAN Program for Calculating Compressible Laminar and Turbulent Boundary Layers in Arbitrary Pressure Gradients. NASA TN D-5681, 1970.
15. Goldman, L. J.; and Seasholtz, R. G.: Laser Anemometer Measurements in an Annular Cascade of Core Turbine Vanes and Comparison with Theory. NASA TP-2018, 1982.
16. Boyle, Robert J.; and Haas, Jeffrey E.: Comparison Between Measured Turbine Stage Performance and the Predicted Performance Using Quasi-Three-Dimensional Flow and Boundary Layer Analysis. To be published.
17. Gelder, T. F.: Aerodynamic Performances of Three Fan Stator Designs Operating with Rotor Having Tip Speed of 337 Meters Per Second and Pressure Ratio of 1.54. I - Experimental Performance. NASA TP-1610, 1980.
18. Gelder, T. F.; Schmidt, J. F.; and Esgar, G. M.: Aerodynamic Performances of Three Fan Stator Designs Operating with Rotor Having Tip Speed of 337 Meters Per Second and Pressure Ratio of 1.54. II - Relation of Analytical Code Calculations to Experimental Performance. NASA TP-1614, 1980.

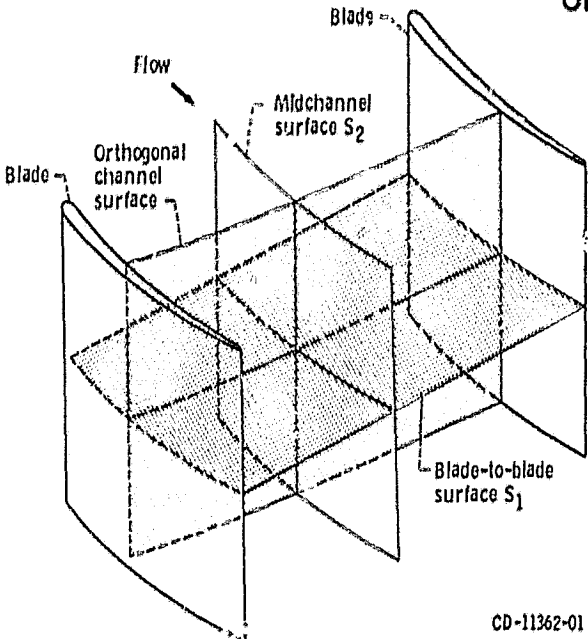


Figure 1, - Two-dimensional analysis surfaces in a turbomachine.

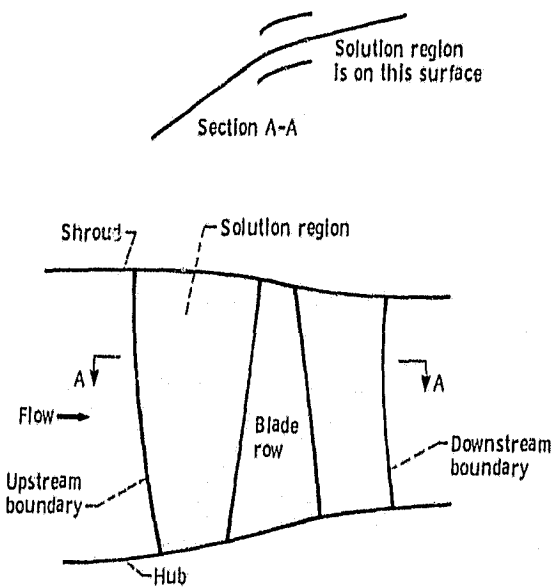


Figure 2, - Solution region.

ORIGINAL PAGE IS
OF POOR QUALITY

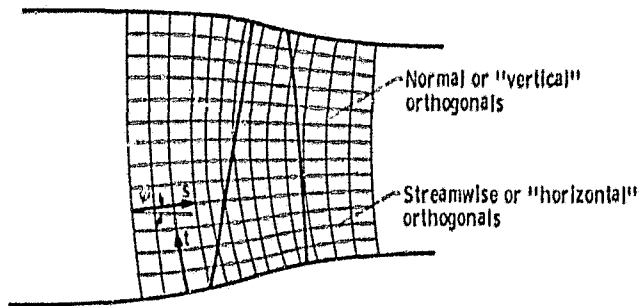


Figure 3. - Orthogonal finite-difference mesh on solution region,

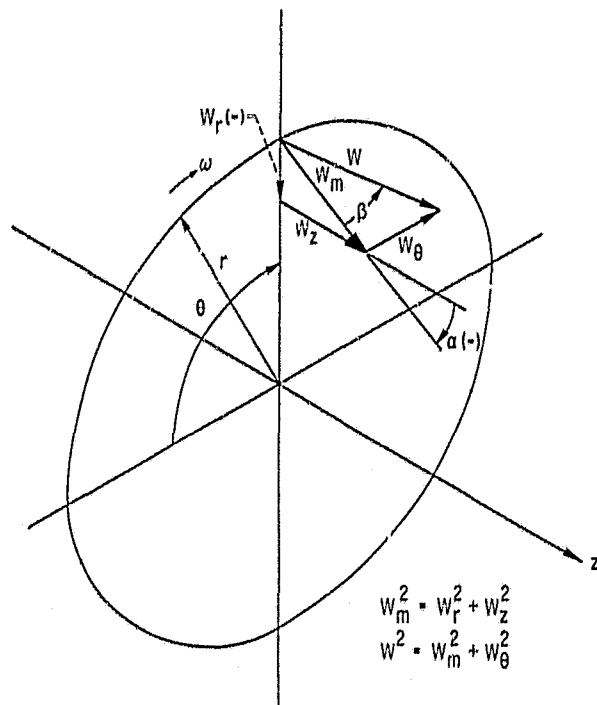


Figure 4. - Cylindrical coordinate system and velocity components,

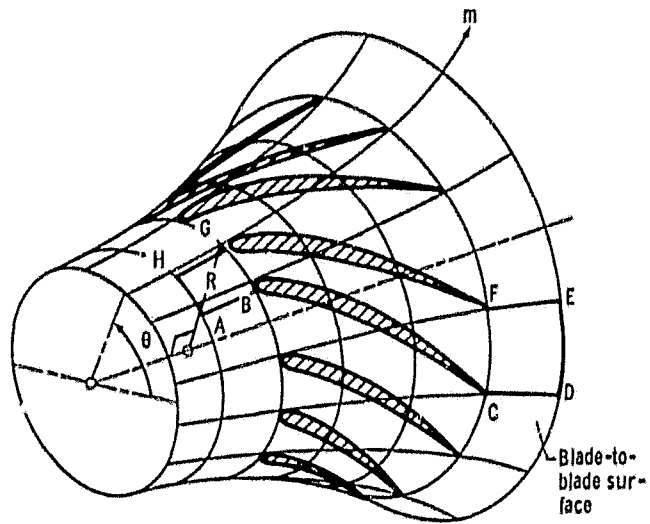


Figure 5. - Blade-to-blade surface of revolution showing $m - \theta$ coordinates.

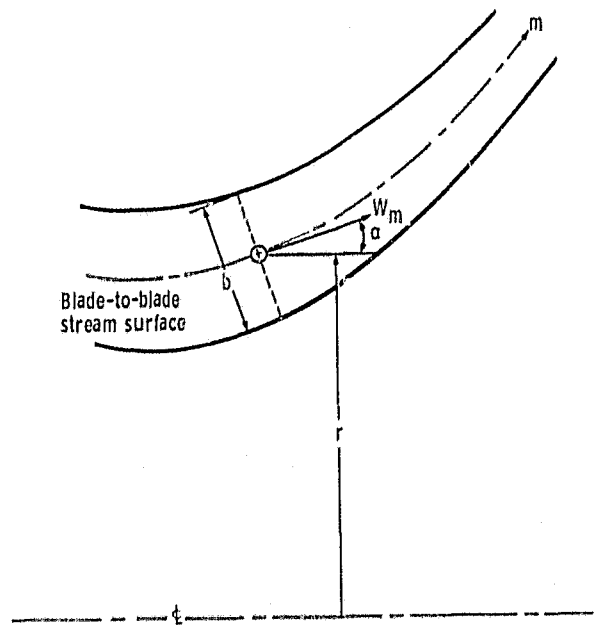


Figure 6. - Flow in a mixed-flow stream channel.

ORIGINAL PAGE IS
OF POOR QUALITY

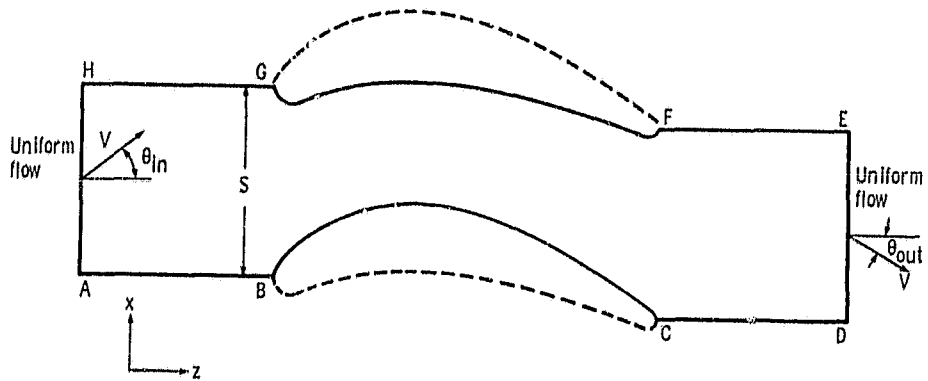


Figure 7. - Finite flow region.

ORIGINAL PAGE IS
OF POOR QUALITY

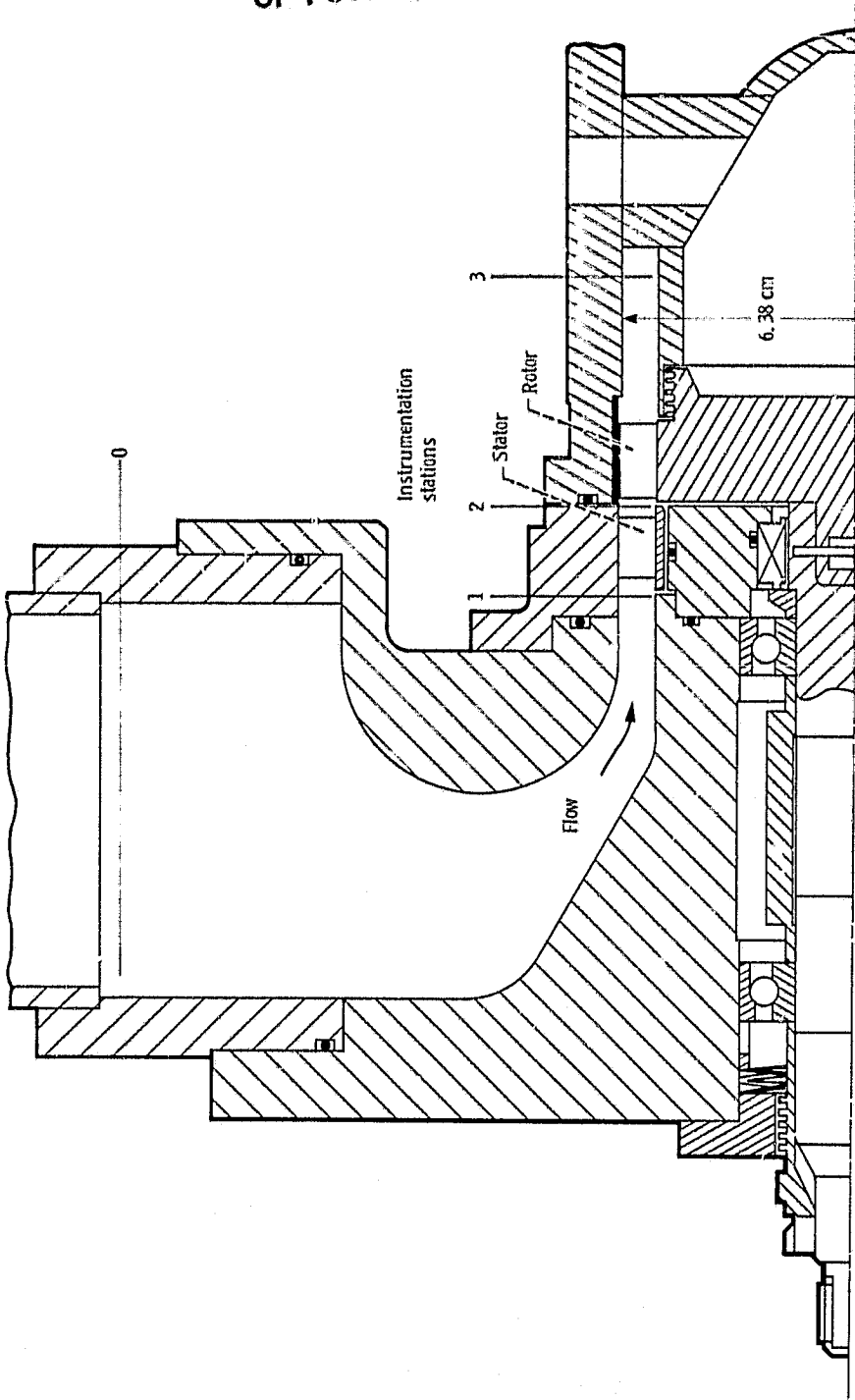


Figure 8. - Cross-sectional view of turbine.

ORIGINAL PAGE 18
OF POOR QUALITY

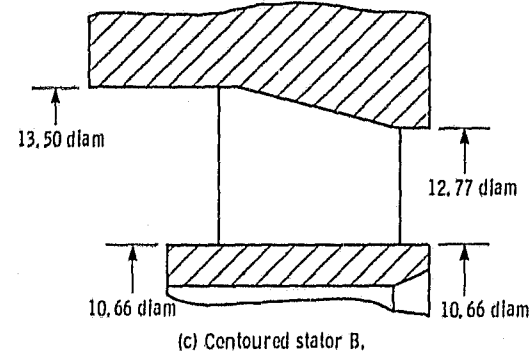
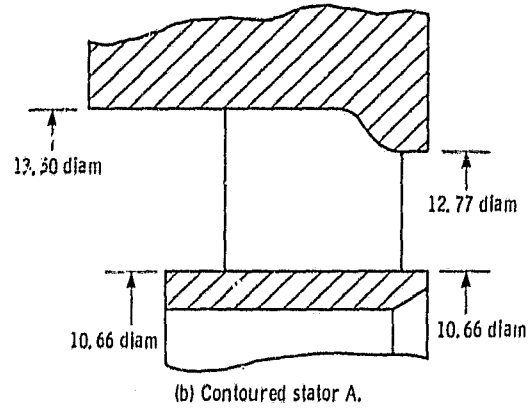
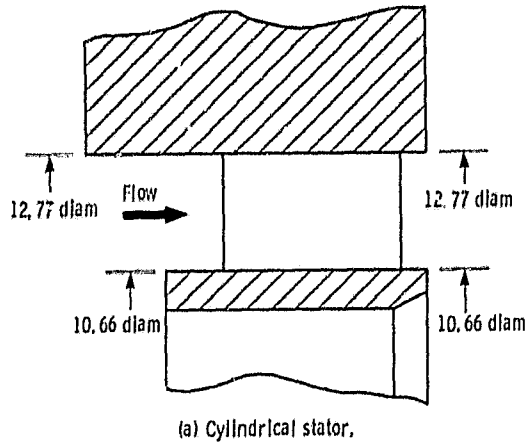


Figure 9. - Schematic cross-sectional view of three stator configurations tested. (Dimensions are in centimeters.)

ORIGINAL PAGE IS
OF POOR QUALITY

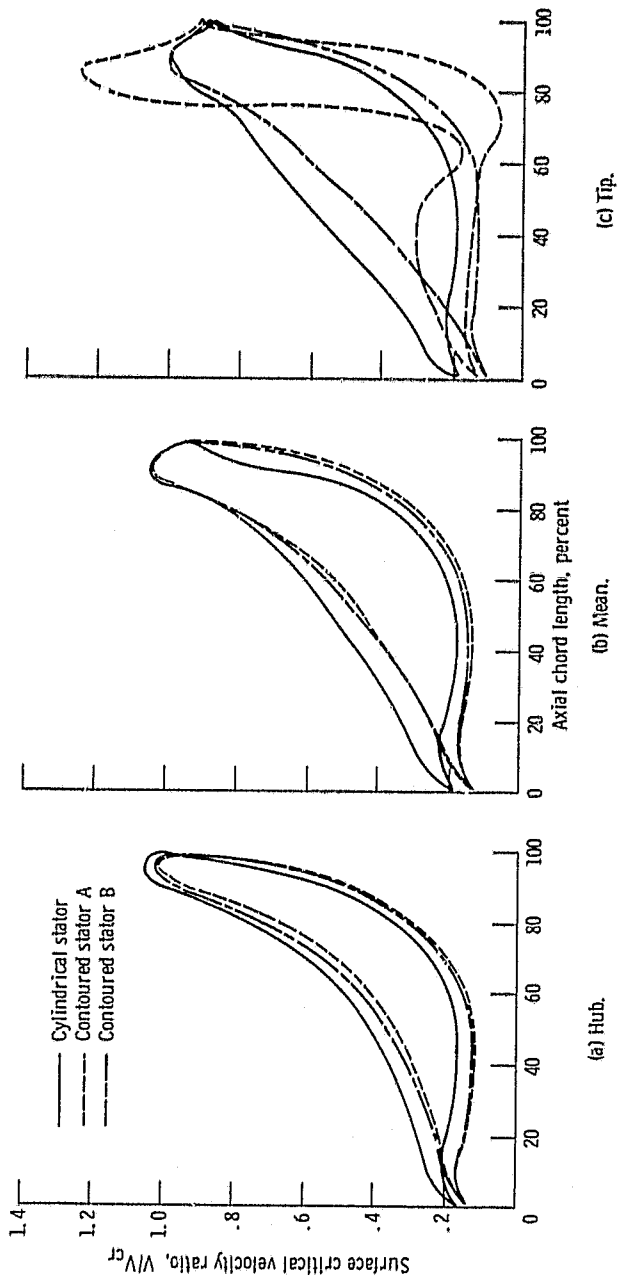


Figure 10. - Design blade surface velocity distributions for the three stator configurations.

ORIGINAL PAGE IS
OF POOR QUALITY

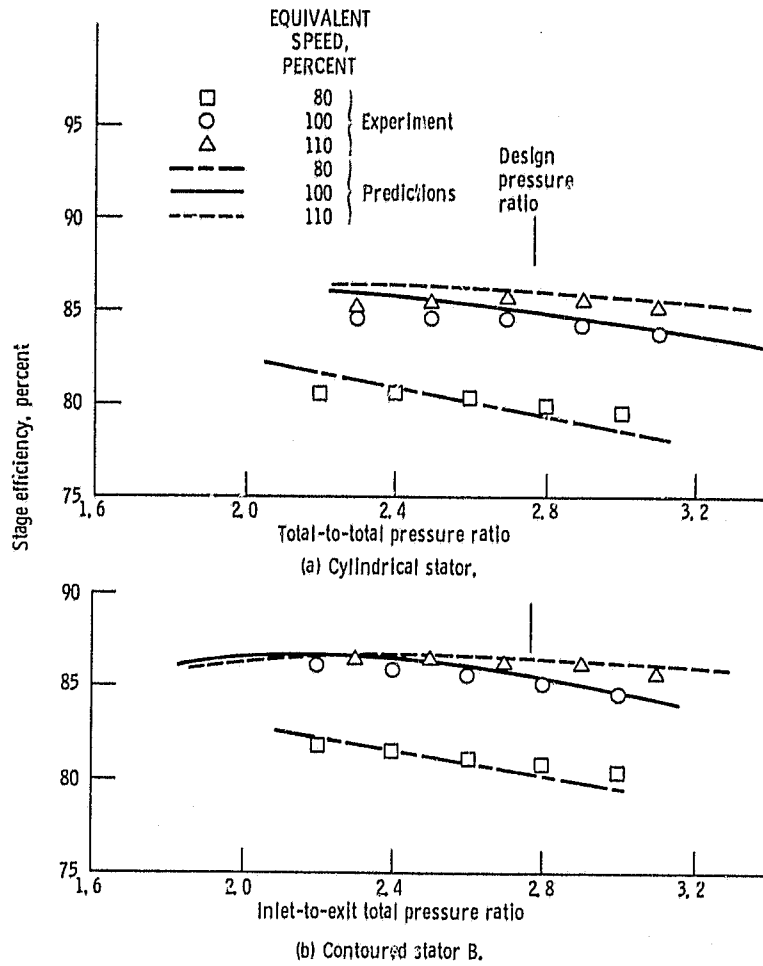


Figure 11. - Comparison between measured and predicted stage efficiency for turbine stage.

ORIGINAL PAGE IS
OF POOR QUALITY

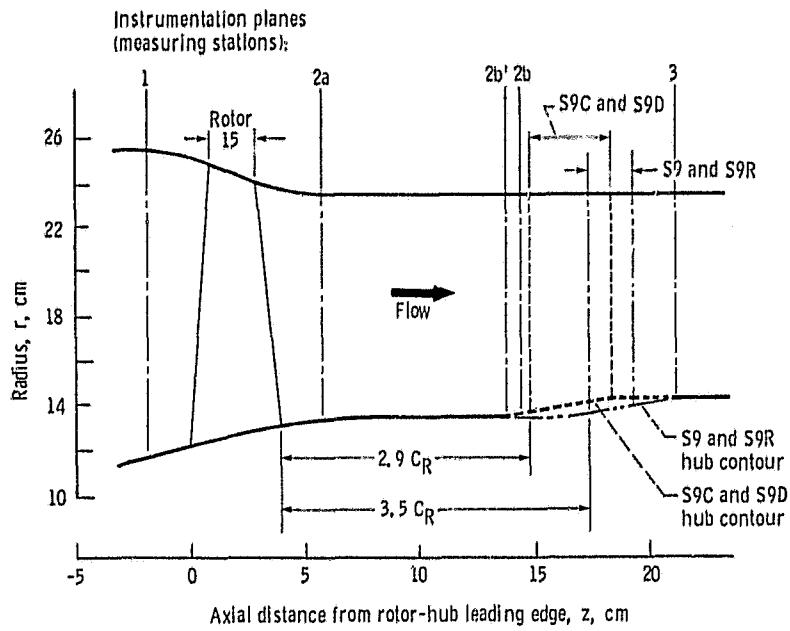


Figure 12 - Flow path for stages showing axial locations of blading and instrumentation.

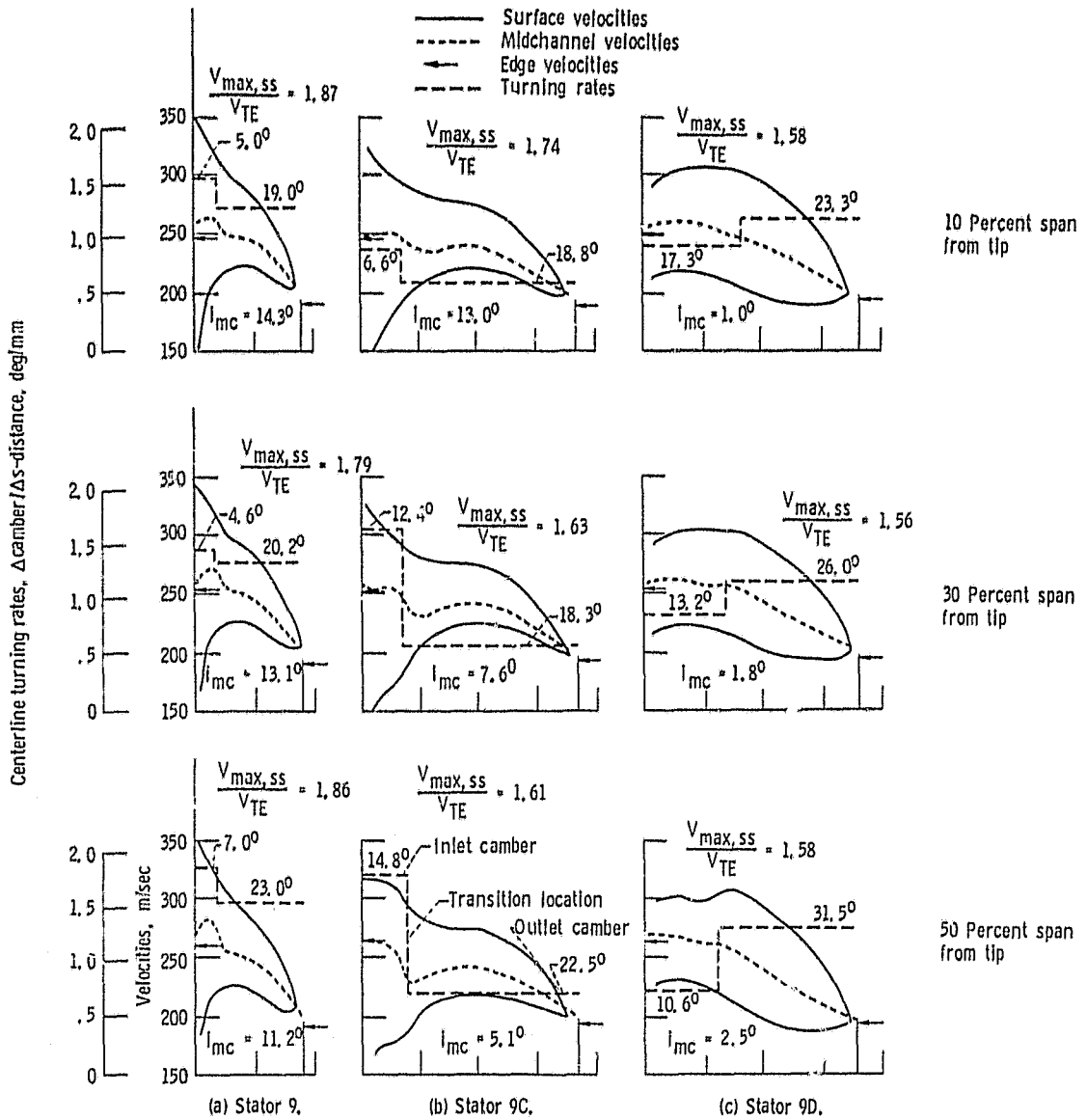


Figure 13. - Chordwise distribution of surface velocities for S9, S9C, and S9D at their design points.

ORIGINAL PAGE IS
OF POOR QUALITY

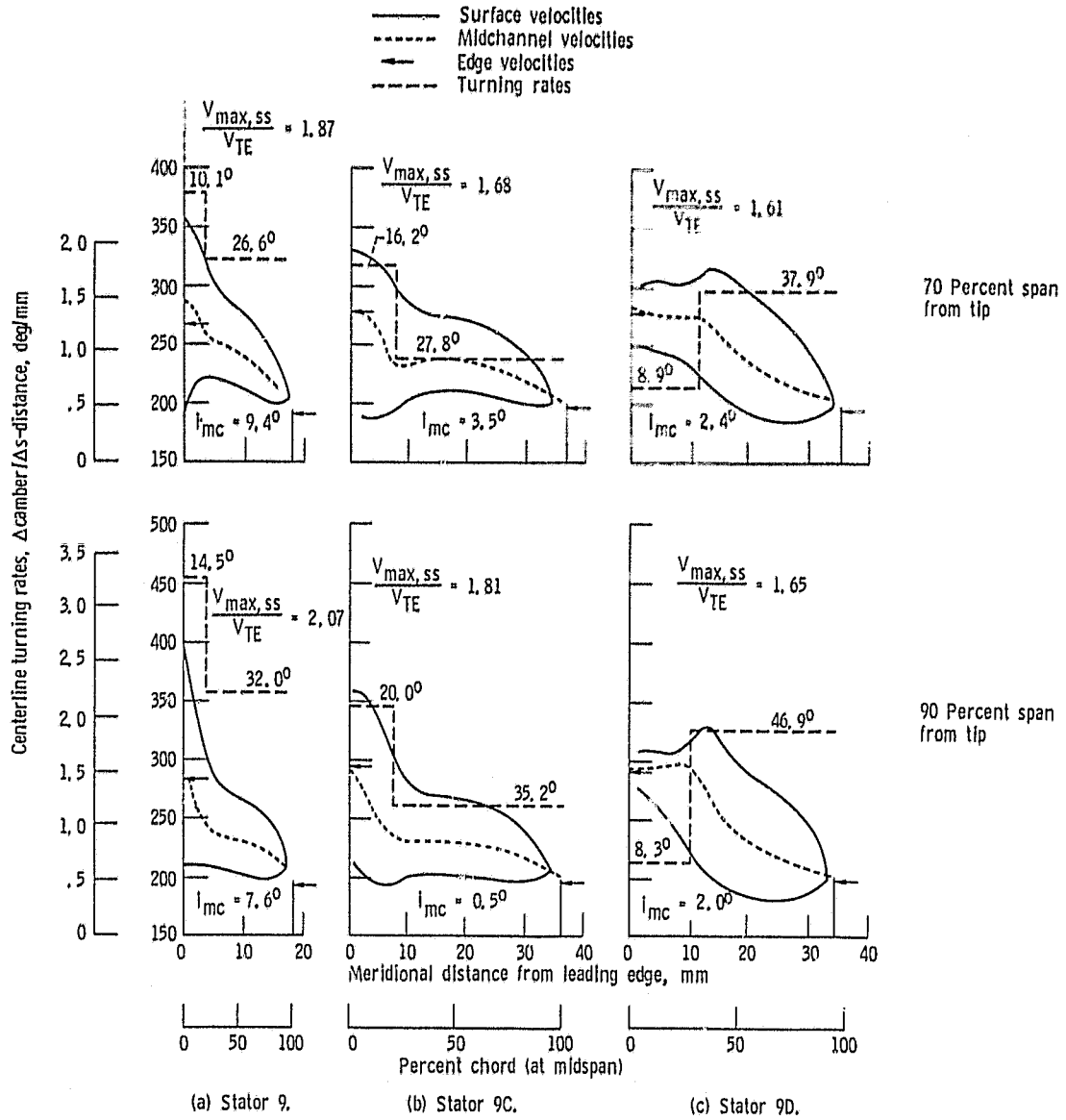


Figure 13. - Concluded.